Cerebral Cortex February 2008;18:424-432
doi:10.1093/cercor/bhm077
Advance Access publication June 7, 2007

Developmental Downregulation of Excitatory GABAergic Transmission in Neocortical Layer I via Presynaptic Adenosine A_1 Receptors

Knut Kirmse, Anton Dvorzhak[1], Rosemarie Grantyn and Sergei Kirischuk

Institute of Neurophysiology, Johannes-Mueller-Center of Physiology, Charité-University-Medicine Berlin, Tucholskystr. 2, 10117 Berlin, Germany
[1]Permanent address: Department of Fundamental and Applied Physiology, Russian States Medical University, Ostrovitjanova 1, 117997 Moscow, Russia

Layer I of the developing cortex contains a dense GABAergic fiber plexus. These fibers provide excitatory inputs to Cajal-Retzius (CR) cells, the early born neurons in layer I. CR cells possess an extensive axonal projection and form synaptic contacts with excitatory, presumably pyramidal, neurons before birth. Interestingly, activity of CR cells declines during the first postnatal week, but mechanism(s) underlying this phenomenon is not yet known. Here we recorded inhibitory postsynaptic currents (IPSCs) in CR cells at postnatal day (P) 1–2 and P5–7. Blockade of adenosine A_1 receptors (A_1Rs) increased the amplitude of evoked IPSCs (eIPSCs) and decreased paired-pulse ratio at P5–7 but not at P1–2. A_1R activation decreased the mean eIPSC amplitude at P5–7, but failed to affect eIPSCs at P1–2. Ecto-adenosine triphosphatase (ATPase) inhibition completely abolished the A_1R-mediated effects suggesting that extracellular ATP is the main source of adenosine. Because A_1R blockade did not affect the median miniature IPSC amplitude, our results demonstrate that adenosine reduces γ-aminiobutyric acid (GABA) release probability via presynaptic A_1Rs at P5–7. As neuronal activity in layer I can depolarize pyramidal neurons influencing thereby glutamatergic synaptogenesis in the lower cortical layers, postnatal weakening of GABAergic transmission by adenosinergic system might reflect a developmental downregulation of this excitatory drive when glutamatergic synapses are formed.

Keywords: ATP release, ecto-ATPase, $GABA_B$, GPCR short-term plasticity

Introduction

Dense, transient γ-aminiobutyric acidergic (GABAergic) fiber plexus confined to layer I is a prominent feature of the developing rodent cortex (Lauder et al. 1986). GABAergic fiber plexus is composed of axons of GABAergic cortical neurons (Marin-Padilla 1998) and extrinsic projections from the zona incerta of the ventral thalamus (Lin et al. 1990). In contrast to the inhibitory GABA action in the adult cortex, GABA has been shown to depolarize neuronal cells in perinatal cortex (Owens et al. 1996; Mienville 1998). Cajal-Retzius (CR) cells, the principal neuronal cell type in the marginal zone/layer I of the developing cortex (Retzius 1893), receive excitatory GABAergic inputs early during development (Kilb and Luhmann 2001). CR cells synthesize and release reelin, an extracellular protein that plays a crucial role in the corticogenesis (for review see Frotscher 1998; Marin-Padilla 1998). However, in addition to reelin synthesis, CR cells are capable to generate action potentials already at birth (Zhou and Hablitz 1996). Moreover, axonal collaterals of CR cells form a horizontally oriented plexus in layer I and project over long (millimeters) distances establishing many synaptic contacts with excitatory neurons, presumably the apical dendrites of pyramidal neurons (Radnikow et al. 2002). Therefore, CR cells are capable to provide an excitatory drive to multiple pyramidal cells in the cortical plate. As many thalamocortical glutamatergic synapses lack synaptic non-N-methyl-D-aspartate (NMDA) receptors and are functionally silent at negative membrane potentials (Isaac et al. 1997), this depolarization may influence glutamatergic synaptogenesis in the lower cortical layers. If this were the case, a decrease of CR cell activity could be expected when glutamatergic synapses have been formed, that is, approximately by the end of the first postnatal week. Indeed, the frequency of both spontaneous inhibitory postsynaptic currents (IPSCs) and Ca^{2+} transients recorded from CR cells in brain slices and isolated whole hemisphere preparations dramatically decreases after P3–4 (Schwartz et al. 1998; Kilb and Luhmann 2001). As the excitability of CR cells does not considerably decrease during the first postnatal week (Zhou and Hablitz 1996), a presynaptic inhibition of excitatory GABAergic inputs can be suggested to underlie the observed reduction in CR cell activity.

Adenosine is a naturally occurring purine nucleoside that regulates many physiological processes (for review see Dunwiddie and Masino 2001; Sawynok and Liu 2003; Fredholm et al. 2005). The endogenous levels of adenosine follow an imbalance between rates of energy consumption and production. Because adenosine tends to reset the energy balance, it has been called a retaliatory metabolite. In addition to its homeostatic role, adenosine is an important neuromodulator, controlling neurotransmitter release and neuronal excitability. Adenosine operates via G-protein–coupled receptors (A_1, A_{2a}, A_{2b}, A_3) that can inhibit (A_1) or enhance (A_2) neuronal communication (for review see Cunha 2001; Ribeiro et al. 2002). The A_1 receptor (A_1R) is ubiquitous within the central nervous system (CNS). High levels of A_1Rs have been shown in the hippocampus, the cerebral cortex, the brain stem, and the spinal cord (for review see Fastbom et al. 1987; Reppert et al. 1991). In the rat CNS, both A_1R messenger RNA and A_1R protein are present already at embryonic day 14 (Rivkees 1995; Weaver 1996). However, the expression of A_1Rs is low in fetuses and increases at birth and during the first 2 postnatal weeks (Geiger et al. 1984; Rivkees 1995; Aden et al. 2001). Moreover, developmental upregulation of A_1Rs is accompanied by an increase of extracellular adenosine concentration (Aranda et al. 1989). Thus, adenosinergic system including both the endogenous agonist and its receptors appears to mature at early postnatal ages and might potentially contribute to the observed developmental suppression of GABAergic inputs to CR cells.

In the present study, GABAergic synaptic currents were recorded from CR cells in mouse brain slices prepared from P1–2 and P5–7 mice. It will be shown that the strength of

excitatory GABAergic synapses on CR cells decreases during the first postnatal week. The observed weakening of GABAergic inputs results from a decrease of GABA release probability by tonically activated presynaptic A_1Rs. We conclude that adenosinergic system reduces the strength of excitatory GABAergic network in layer I during the first postnatal week and might contribute to developmental elimination of excitatory GABAergic network in layer I.

Materials and Methods

Brain Slices Preparation

All experiments were conducted with pigmented C57BL/6J mice pups of postnatal days (P) 1–2 and 5–7 (the day of birth was designated as P0). Animals were decapitated under deep ether anesthesia. The brain was removed quickly and transferred into ice-cold saline that contained (in mM): 125 NaCl, 4 KCl, 10 glucose, 1.25 NaH_2PO_4, 25 $NaHCO_3$, 0.5 $CaCl_2$, and 2.5 $MgCl_2$ constantly aerated with a 5% CO_2/95% O_2 mixture (pH = 7.3). The brain was separated into 2 hemispheres. Sagittal slices of both hemispheres were cut on a vibratome (Integraslice 7550PSDS, Campden Instruments Ltd., Loughborough, UK). Visual cortex areas 17 and 18 were identified based on the stereotaxic atlas of the mouse brain. After preparation, slices (200 μm thick) were stored for at least 1 h at room temperature in artificial cerebrospinal fluid (ACSF) that contained (in mM): 125 NaCl, 4 KCl, 10 glucose, 1.25 NaH_2PO_4, 25 $NaHCO_3$, 2 $CaCl_2$, and 1 $MgCl_2$. pH was buffered to 7.3 by continuous bubbling with a 5% CO_2/95% O_2 mixture. The osmolarity was 330 mOsm. All experiments were carried out according to the guidelines laid down by the Office of Health Protection and Technical Safety of the regional government Berlin (Landesamt für Arbeitsschutz, Gesundheitsschutz und technische Sicherheit Berlin, T0406/03).

Electrophysiological Recordings in Acute Slices

For recordings, slices were placed into a recording chamber (~0.4 ml volume) on the microscope stage (Axioscope FS, Zeiss, Oberkochen, Germany) equipped with phase contrast optics. Slices were submerged with a constant flow of oxygenated ACSF. Ten micromolar 6,7-dinitroquinoxaline-2,3-dione (DNQX, an AMPA/kainate receptor antagonist) and 50 μM DL-2-amino-5-phosphonopentanoic acid (a NMDA receptor blocker) were added to the ACSF to block glutamatergic currents, unless otherwise stated. Flow rate was set to 1 mL/min using a gravity-driven manually operated superfusion system. A ×40 water immersion objective (Zeiss, Oberkochen, Germany) was used in all experiments. IPSCs were recorded using the whole-cell configuration of the patch-clamp technique. Intrapipette solution contained (in mM): 100 potassium gluconate, 50 KCl, 5 NaCl, 0.5 $CaCl_2$, 5 ethyleneglycol-bis(2-aminoethylether)-*N*,*N*,*N*′,*N*′-tetraacetic acid, 25 4-(2-hydroxyethyl)-1-piperazineethanesulfonic acid, 2 Mg-adenosine triphosphate (ATP), 0.3 guanosine triphosphate, pH was set to 7.2 with KOH. The osmolarity was 320 mOsm. Pipette resistance was 3–5 MΩ, when filled with the above saline. Liquid junction potentials (<5 mV) were not corrected. Electrophysiological signals were acquired using an EPC-7 amplifier (List, Darmstadt, Germany), a 16-bit AD/DA board (ITC-16, HEKA Elektronik, Lambrecht, Germany), and TIDA 4.11 software (HEKA Elektronik). The signals were filtered at 3 kHz and sampled at a rate of 10 kHz.

Access resistance was controlled by applying hyperpolarizing pulses of 10 mV. Cell capacitance and access resistance values were obtained by fitting a monoexponential function to the capacitance artifacts. Only recordings with a series resistance below 40 MΩ were accepted. Series resistance compensation was not applied. Cells exhibiting more than 20% changes in the access resistance during an experiment were discarded. The chloride reversal potential was about −20 mV. The holding potential was set to −70 mV.

CR Cell Identification

The identification of CR cells in the mouse visual cortex was described elsewhere (Hestrin and Armstrong 1996; Radnikow et al. 2002). Briefly, CR cells were visually selected according to morphological criteria: 1) location in layer I, 2) horizontal orientation, 3) large ovoid soma, and 4) one thick tapered dendrite typically extended in parallel to the pial surface. Electrophysiologically, CR cells have been shown to exhibit 1) a relatively depolarized resting potential (Mienville and Pesold 1999), and 2) a hyperpolarization-activated inward I_h current (Kilb and Luhmann 2000).

Spontaneous synaptic currents in CR cells were completely and reversibly blocked by 10 μM bicuculline methiodide (n = 15) or 20 μM gabazine (n = 5) revealing their GABAergic nature (data not shown; Kirmse and Kirischuk 2006a). In the present study, $GABA_A$ receptor-mediated postsynaptic currents will be referred to as IPSCs even though the action of GABA is depolarizing in CR cells (Mienville 1998). Miniature IPSCs (mIPSCs) were recorded in the presence of tetrodotoxin (TTX) (1 μM).

Electrical Stimulation

Evoked postsynaptic currents were elicited by focal electrical stimulation through a glass pipette filled with ACSF (about 10 MΩ). In this case, *N*-(2,6-dimethylphenylcarbamoylmethyl)-triethylammonium bromide (QX 314, 2 mM) was added to the intracellular solution to prevent generation of action potentials in the tested neurons (Connors and Prince 1982). An isolated stimulation unit was used to generate rectangular electrical pulses. Pulse duration was set to 0.5 ms. Pulse intensity was adjusted to activate a unitary synaptic input (minimal stimulation). Simulation was accepted as minimal if the following criteria were satisfied: 1) evoked IPSC (eIPSC) latency remained stable (<20% fluctuations); 2) lowering stimulus intensity by 20% resulted in a complete failure of eIPSCs; 3) an increase in stimulus intensity by 20% changed neither mean eIPSC amplitude nor eIPSC shape. Typical pulse intensity required for minimal stimulation was between 1 and 2 μA.

To estimate the size of the readily releasable pool (RRP), we used high frequency stimulation (Schneggenburger et al. 1999; Lu and Trussell 2000; Kirischuk and Grantyn 2003). Repetitive stimulation leads to a decrease in the eIPSC amplitudes. Assuming that the eIPSC depression is largely caused by a transient decrease in the number of readily releasable quanta, it is possible to estimate the RRP size on the basis of cumulative eIPSC amplitude plot (Schneggenburger et al. 1999; Lu and Trussell 2000; Kirischuk and Grantyn 2003). Namely, cumulative eIPSC amplitudes were plotted versus stimulus number. Because repetitive stimulation causes a compound postsynaptic response (synchronous and asynchronous), IPSCs that peaked within a 3-ms interval following the end of a stimulus pulse were selected as stimulus-locked eIPSCs (Kirischuk and Grantyn 2003). After 10–20 pulses, the cumulative eIPSCs reached a steady state, as indicated by the linear slope dependence of the cumulative eIPSC amplitude on the pulse number. Assuming that 1) the number of release sites remains constant throughout the experiment and 2) the linear component reflects vesicle recycling, the cumulative IPSC amplitude in the absence of pool replenishment can be estimated by back-extrapolation to the start of the train. Note that RRP estimations were performed without preceding or following mIPSC measurements. Therefore, the RRP in this work has a dimension of pA and represents the product of the number of release sites and the quantal amplitude. Release probability (p_r) was calculated using the binomial model approximation, namely, p_r = mean eIPSC/RRP. Stimulation trains of 40 pulses delivered at 20 Hz were applied to obtain RRP estimates (Kirmse and Kirischuk 2006a).

Superfusion

All experiments were performed at room temperature (22–25 °C), unless otherwise stated (Fig. 3). TTX was obtained from Alomone Labs (Jerusalem, Israel). (2*S*)-3-[[(1*S*)-1-(3,4-dichlorophenyl)ethyl]amino-2-hydroxypropyl] (phenylmethyl)phosphinic acid (CGP55845) and 8-cyclopentyl-1,3-dipropylxanthine (DPCPX) were from Tocris (Bristol, UK). All other chemicals were obtained from Sigma-Aldrich (Munich, Germany).

Data Evaluation and Statistics

Data were evaluated off-line using PeakCount V3.2 software (C. Henneberger, Institute of Neurophysiology, Berlin). The program employs a derivative threshold-crossing algorithm to detect individual mIPSCs. Each automatically detected event is displayed for visual inspection. mIPSC rise times and decay time constants (a single

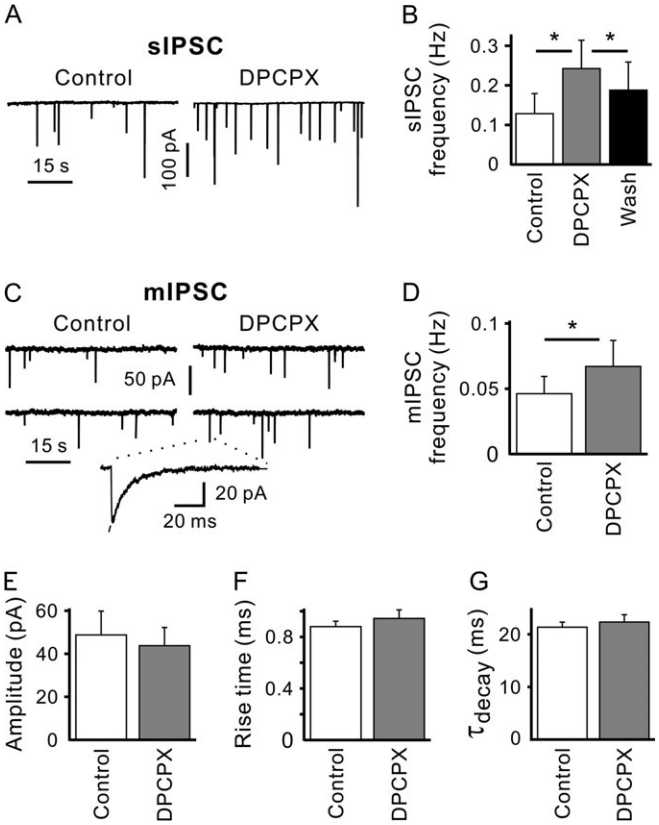

Figure 1. Functional A_1Rs are located presynaptically in GABAergic boutons on CR cells at P5–7. (*A*, *B*) DPCPX (1 μM) induced an increase of spontaneous IPSC frequency. Sample recordings (*A*) and statistical data obtained from 6 CR cells (B). (*C*, *D*) A_1R blockade increased mIPSC frequency. Sample recordings (*C*) and statistical data (*D*, $n = 6$). The inset shows and individual mIPSC with a monoexponential fit of decay. (*E–G*) DPCPX modified neither the median amplitude (*E*), nor the mean rise time (*F*), nor the decay time constant (*G*) of mIPSCs. Data obtained from 6 CR cells. * shows a significant difference ($P < 0.05$).

exponential fit, Fig. 1*C* the inset) can be also obtained. All results are presented as mean ± SEM. The error bars in all figures indicate standard error of the mean (SEM). Differences between means were tested for significance using paired Student's *t*-test, unless otherwise stated.

Results

Presynaptic Location of Functional Adenosine A_1 Receptors (A_1Rs) at P5–7

To examine whether A_1Rs contribute to immature network activity, we applied DPCPX, a specific A_1R antagonist. DPCPX (1 μM) significantly increased spontaneous IPSC frequency, and this effect was partially reversible. The corresponding frequencies were 0.13 ± 0.05, 0.24 ± 0.07, and 0.18 ± 0.07 Hz in the control, in the presence and after the washout of DPCPX, respectively ($P < 0.05$, $n = 6$, Fig. 1*A,B*). A_1R blockade also increased the mean amplitude of spontaneous IPSCs from 71 ± 14 to 99 ± 20 pA ($P < 0.05$, $n = 6$). Because DPCPX changed neither the mean holding current (−30 ± 20 and −20 ± 20 pA, $n = 6$, $P > 0.5$) nor the membrane resistance (790 ± 110 and 750 ± 140 MΩ in control and in the presence of DPCPX, respectively, $n = 6$, $P > 0.3$, data not shown), these results demonstrate that in the neocortical layer I A_1Rs are functional and located presynaptically.

To corroborate the suggestion, miniature IPSCs (mIPSCs) were recorded in the presence of TTX (1 μM), a specific blocker of voltage-sensitive Na^+ channels. DPCPX increased mIPSC frequency from 0.05 ± 0.01 Hz to 0.07 ± 0.02 Hz ($P < 0.05$, $n = 6$, Fig. 1*C,D*), but influenced neither the median mIPSC amplitude (48 ± 11 and 44 ± 9 pA, $P > 0.2$, Fig. 1*E*), nor the mean mIPSC rise time (0.89 ± 0.04 and 0.94 ± 0.06 ms, $P > 0.35$, Fig. 1*F*), nor the mean decay time constant of mIPSCs (21 ± 2 and 22 ± 3 ms in control and in the presence of DPCPX, respectively, $P > 0.3$, $n = 6$, Fig. 1*G*). These data confirm the presynaptic location of A_1Rs.

A_1R Blockade Increases GABA Release Probability at P5–7

Next, we studied whether A_1Rs contribute to short-term plasticity at GABAergic synapses on CR cells. eIPSCs were elicited by minimal electrical stimulation in layer I using a paired-pulse protocol (20 Hz). The intertrial interval was set to 10 s. The mean eIPSC amplitude was significantly increased from 94 ± 27 in control to 144 ± 34 pA in the presence of DPCPX ($P < 0.01$, $n = 10$, Fig. 2*A,B*). This DPCPX effect was slowly (about 30 min washout time) reversible (Fig. 2*B*). In addition to the DPCPX-induced increase of the mean eIPSC amplitude, A_1R blockade significantly decreased the paired-pulse ratio (PPR, mean $eIPSC_2$/mean $eIPSC_1$). DPCPX diminished PPR from 1.6 ± 0.2 to 0.9 ± 0.1 ($P < 0.001$, $n = 10$) and this effect was partially reversible (Fig. 2*A,C*). We also asked if A_1R blockade influences the size of the RRP. The latter was estimated using a 20 Hz train of 40 pulses (see Methods and Kirmse and Kirischuk 2006a, Fig. 2*D,E*). Figure 2*F* shows that DPCPX did not change the RRP size. The corresponding values were 714 ± 302 and 684 ± 274 pA ($P > 0.45$, $n = 10$). Lack of DPCPX effect on the median mIPSC amplitude (Fig. 1*E*) and the RRP size suggests that the DPCPX influences GABA release probability. In the frame of the binomial model of synaptic transmission the mean amplitude of $eIPSC_1$ is equal to the product of *RRP* and release probability (p_r). Consequently, one can calculate GABA release probability. The corresponding values were 0.13 ± 0.02 in control and 0.23 ± 0.04 in the presence of DPCPX ($P < 0.01$, $n = 10$, Fig. 2*G*).

To inspect whether A_1R-mediated effects are due to a decreased metabolic rate at room temperature, we performed experiments at near-physiological (34 °C) temperature. DPCPX reduced PPR also under these conditions (Fig. 3*A,B*). The corresponding PPR values were 1.24 ± 0.15 and 0.97 ± 0.11 in control and in the presence of DPCPX ($P < 0.05$, $n = 7$, Fig. 3*B*). Calculated release probabilities were 0.15 ± 0.01 and 0.20 ± 0.01 ($P < 0.01$, $n = 7$, Fig. 3*B*). We conclude that presynaptic A_1Rs are activated also at near-physiological temperatures and inhibit GABA release.

Presynaptic A_1Rs are Partially Activated by Ambient Adenosine at P5–7

The observation that DPCPX, a specific A_1R blocker, increased the probability of GABA release suggests that A_1Rs are at least partially activated under control conditions. To examine the degree of A_1R activation, we aimed at maximal activation of A_1Rs by applying N^6-cyclopentyladenosine (CPA), a specific A_1R agonist. Like DPCPX, CPA (1 μM) influenced neither the holding current nor the membrane resistance (data not shown) confirming the presynaptic location of A_1Rs. However, CPA significantly decreased the mean eIPSC amplitude to 74 ± 8%

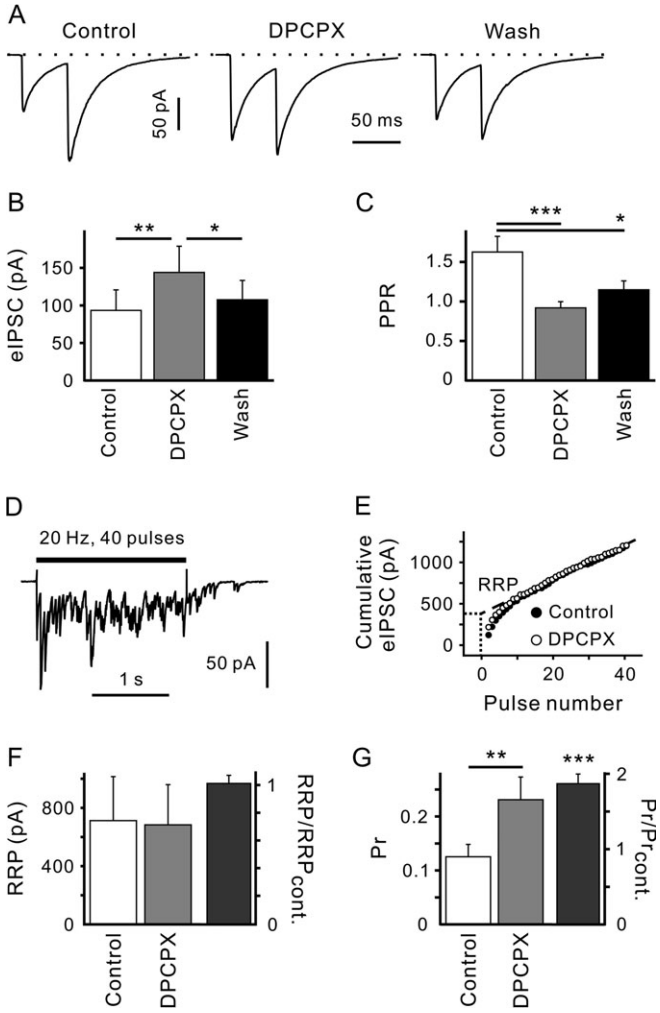

Figure 2. Presynaptic A_1Rs control GABA release probability at P5–7. (*A*) Sample traces show paired-pulse–elicited eIPSCs recorded in control, in the presence and after washout of DPCPX. Traces represent an average of 40 sequential responses. Data obtained from the same cell. (*B*, *C*) DPCPX reversibly increased the mean amplitude of eIPSCs (*B*) and decreased the PPR (C, $n = 10$). (*D*, *F*) DPCPX failed to affect the RRP size. (*D*) Sample trace shows an averaged postsynaptic response (5 trials) elicited by a 40 stimuli train delivered at 20 Hz. (*E*) Cumulative amplitude plots in the presence (open symbols) and absence (filled symbols) of DPCPX. SEMs are not shown for clarity. To obtain the RRP estimates, the last 20 points (from 21st to 40th pulses) were fitted by linear regression (dashed line), and back-extrapolated to time 0 (see Methods). (*F*) DPCPX did not change the RRP size ($n = 10$). (*G*) DPCPX drastically increased GABA release probability. The latter was calculated as the ratio of the mean eIPSC amplitude to the RRP size. *, ** and *** show $P < 0.05$, <0.01, and 0.001, respectively.

($P < 0.01$) and increased the PPR to 150 ± 12% ($P < 0.01$, $n = 13$, one population Student's *t*-test, Fig. 4*A,B*). DPCPX applied after CPA washout (30 min) led to an increase in the mean eIPSC amplitude and decrease of PPR (Fig. 4*C,D*). These data suggest that under control conditions A_1Rs are only partially activated by ambient adenosine. Consequently, changes in extracellular adenosine concentration can dynamically alter the strength of GABAergic synapses on CR cells at P5–7.

Immaturity of A_1Rs at P1–2

Maturation of adenosine A_1R signaling in the CNS occurs at early postnatal ages (Aden et al. 2001). Therefore, we asked if the A_1R-mediated inhibition of GABAergic synapses on CR cells also exists at P1–2. Figure 5*A,B* shows that DPCPX only slightly increased the mean amplitude of eIPSCs to 109 ± 9% ($P = 0.32$) and decreased PPR to 94 ± 5% ($P = 0.22$, $n = 12$, one population

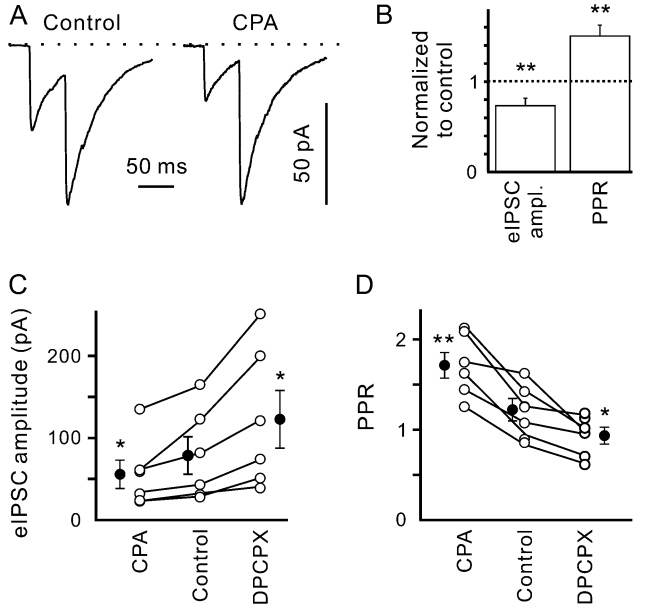

Figure 4. Presynaptic A_1Rs receptors are only partially activated under control conditions at P5–7. (*A*) Paired-pulse–induced eIPSCs in control and in the presence of CPA (1 μM). Traces represent an average of 40 sequential responses. (*B*) CPA significantly decreased the mean amplitude of eIPSCs and increased the PPR ($n = 13$). (*C*, *D*) The mean eIPSC amplitudes (*C*) and PPRs (*D*) obtained in control and in the presence of either CPA or DPCPX for each individual cell. Filled symbols show the respective mean values ($n = 6$). Symbols * and ** mean $P < 0.05$ and <0.01, respectively.

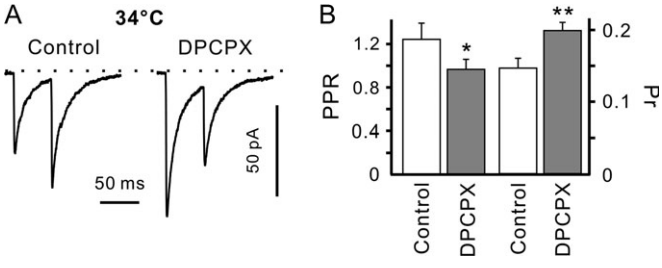

Figure 3. Presynaptic A_1Rs are activated at near-physiological temperature. (*A*) Paired-pulse eIPSCs recorded at 34 °C in control and in the presence of DPCPX. (*B*) At near-physiological temperature, DPCPX significantly decreased the PPR and increased GABA release probability (Pr, $n = 7$). Symbols * and ** mean $P < 0.05$ and <0.01, respectively.

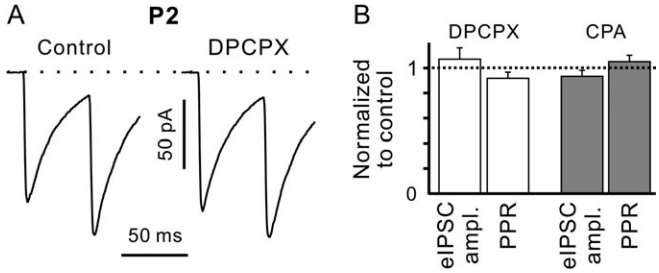

Figure 5. Presynaptic A_1Rs are not expressed or not functional at P1–2. (*A*) Paired-pulse–induced eIPSCs in control and in the presence of DPCPX (1 μM). Traces represent an average of 40 sequential responses. (*B*) Both DPCPX (left, $n = 12$) and CPA (right, $n = 6$) failed to alter the mean amplitude of eIPSCs or PPR in P1–2 slices.

Student's *t*-test). The inefficiency of DPCPX may either result from low density of A_1Rs on presynaptic terminals or low extracellular concentration of adenosine. To distinguish between these possibilities, we performed experiments aimed to fully activate A_1Rs. CPA decreased the mean amplitude of eIPSCs to 94 ± 5% ($P = 0.08$) and increased PPR to 107 ± 5% ($P = 0.07$, $n = 6$, one population Student's *t*-test, Fig. 5*B*). Because CPA effects were not statistically significant, we conclude that presynaptic A_1Rs are either not expressed or not functional at P1–2.

Extracellular ATP Degradation is the Main Source of Ambient Adenosine

Next, we investigated the mechanisms that control extracellular adenosine concentration at P5–7. Firstly, adenosine can be formed inside the cell from ATP by intracellular 5′-nucleotidase and then transported outside the cell via bidirectional adenosine transporters (Deckert et al. 1988). The latter can be blocked by dipyridamole, a broad spectrum adenosine transport inhibitor. In this study, dipyridamole (10 μM) influenced neither the mean eIPSC amplitude (96 ± 8% of control, $P > 0.6$) nor the PPR (107 ± 9%, $P > 0.2$, one population Student's *t*-test, $n = 5$, Fig. 6*A,B*). These data show that in this preparation equilibrative

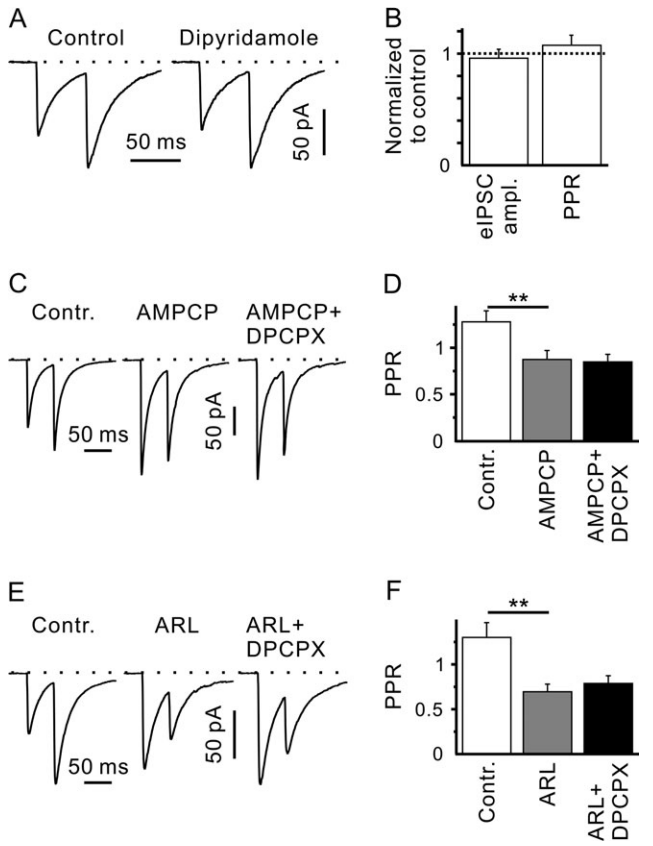

Figure 6. Extracellular ATP is the main source of ambient adenosine. (*A*, *B*) Sample traces and statistical data ($n = 5$) show that dipyridamole (10 μM), an adenosine transport inhibitor, affected neither the mean eIPSC amplitude nor the PPR. (*C*, *D*) Sample traces and statistical data show that AMPCP (100 μM), an ecto-5′-nucleotidase inhibitor, significantly decreased PPR ($n = 5$). Note that DPCPX was not effective when applied in the presence of AMPCP. (*E*, *F*) Sample traces and statistical data ($n = 6$) show that ARL-67156 (50 μM), a specific ecto-ATPase inhibitor, significantly decreased PPR. Note that DPCPX was not effective when applied in the presence of ARL-67156. ** shows a significant difference ($P < 0.01$).

adenosine transporters are not the main mechanism that regulates extracellular adenosine concentration.

Secondly, adenosine can be generated outside the cell by the metabolism of released nucleotides by ecto-nucleotidases. There is a family of ecto-nucleotidases that can generate adenosine, but ecto-5′-nucleotidase is the major enzyme responsible for this under physiological conditions (Zimmermann 2000). Ecto-5′-nucleotidase can be blocked by adenosine 5′-α,β-methylene-diphosphate (AMPCP). Application of AMPCP (100 μM) resulted in an increase of the mean eIPSC amplitude (99 ± 34 and 145 ± 64 pA, $n = 5$, $P < 0.01$) and decrease of the PPR (1.28 ± 0.11 and 0.87 ± 0.09 in control and in the presence of AMPCP, respectively, $P < 0.01$, $n = 5$, Fig. 6*C,D*). Moreover, in the presence of AMPCP DPCPX failed to affect either the mean eIPSC amplitude (145 ± 64 and 144 ± 57 pA, $P > 0.3$) or the PPR (0.87 ± 0.09 and 0.85 ± 0.08 in the presence of AMPCP and AMPCP plus DPCPX, respectively, $P > 0.8$, $n = 5$, Fig. 6*C,D*). These data suggest that endogenous adenosine is mainly generated extracellular through a conversion of released nucleotides.

To corroborate this observation, we applied exogenous ATP. ATP (100 μM) increased the PPR from 1.2 ± 0.2 to 1.8 ± 0.3 ($n = 4$, $P < 0.05$), but was ineffective in the presence of DPCPX. The corresponding PPR values were 0.53 ± 0.07 and 0.55 ± 0.09 in the presence of DPCPX and DPCPX plus ATP, respectively ($n = 5$, $P > 0.4$, data not shown). These data show that exogenous ATP leads to A_1R activation in this preparation. To inspect the possibility that ATP is the main precursor of ambient adenosine, we applied 6-*N,N*-diethyl-D-β,γ-dibromomethylene-ATP (ARL-67156), a specific inhibitor of ecto-ATPase (Crack et al. 1995). ARL-67156 (50 μM) decreased the PPR from 1.3 ± 0.2 to 0.7 ± 0.1 ($P < 0.01$, $n = 6$, Fig. 6*E,F*). Moreover, DPCPX applied in the presence of ARL-67156 failed to produce significant changes in the PPR (0.7 ± 0.1 and 0.8 ± 0.1 in the presence of ARL-67156 and ARL-67156 plus DPCPX, respectively, $P > 0.2$, $n = 6$, Fig. 6*E,F*). In addition, AMPCP was also ineffective in the presence of ARL-67156. The corresponding PPR values were 0.78 ± 0.07 and 0.82 ± 0.06 in the presence of ARL-67156 and ARL-67156 plus AMPCP, respectively ($P > 0.4$, $n = 4$, data not shown). These results suggest that extracellular adenosine is mostly generated via ecto-ATPase–mediated degradation of extracellular ATP.

Activation of Presynaptic A_1Rs Is Not Mediated by Synaptically Released ATP

GABA and ATP have been shown to be coreleased in the spinal cord (Jo and Schlichter 1999; Hugel and Schlichter 2003) and in the hypothalamus (Jo and Role 2002). In addition, in the hippocampus extracellular ATP has been shown to be converted to adenosine with a $T_{½}$ of 200 ms (Dunwiddie et al. 1997) suggesting that it could contribute to the A_1R-mediated short-term plasticity. To examine this hypothesis, we performed the following experiments. To prevent an activity-dependent contribution of $GABA_B$Rs (Kirmse and Kirischuk 2006a), 1 μM CGP55845, a selective $GABA_B$R antagonist, was added to ACSF. Firstly, we applied paired-pulse stimulation with variable interstimulus intervals (ISIs) and inspected DPCPX effects on the PPR at long (250–1000 ms) ISIs. Figure 7*A,B* shows that paired-pulse behavior was not sensitive to DPCPX ($n = 5$). Secondly, we investigated the relationship between the first and the second eIPSC in individual pairs recorded at the ISI of 250 ms. If ATP is coreleased with GABA and contributes to the A_1R-mediated inhibition of release, a larger $eIPSC_1$ should be followed by a

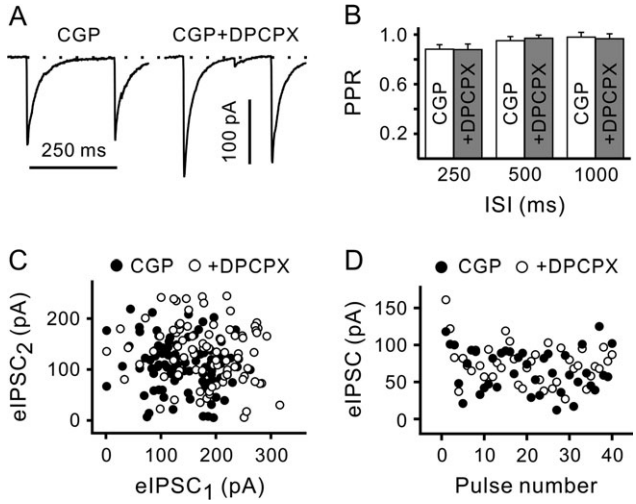

Figure 7. A_1R-mediated inhibition of GABA release does not depend on synaptic activity. (*A*) Paired-pulse–induced eIPSCs in the presence of CGP55845 (CGP, 1 μM) and CGP55845 plus DPCPX. Traces represent an average of 40 sequential responses. ISI was set to 250 ms. (*B*) Statistical data show that in the presence of CGP55845 DPCPX did not significantly affect PPR at long ISIs (n = 5–8). (*C*) Plots of the second eIPSC amplitude against the first eIPSC amplitude in individual pairs in the presence of CGP55845 (filled symbols) and CGP55845 plus DPCPX (open symbols). Data obtained from a single CR cell. (*D*) Dependence of eIPSC amplitudes on the pulse number during 4-Hz stimulation in the presence of CGP55845 (filled symbols) and CGP55845 plus DPCPX (open symbols). Each point is an average of 5 sequential responses. SEMs are not shown for clarity. Data obtained from the same CR cell.

smaller $eIPSC_2$, that is, their amplitudes should demonstrate a negative correlation. However, no correlation was observed either in the presence of CGP55845 or in the presence of CGP55845 plus DPCPX (n = 4, minimal P > 0.4, Fig. 7*C*). Thirdly, we applied low frequency (4 Hz, 40 pulses) stimulation. If ATP is coreleased, adenosine concentration at synaptic sites should rise up resulting in tetanic depression of eIPSC amplitudes during trains. Figure 7*D* shows that DPCPX did not affect eIPSC amplitudes elicited by 4 Hz trains (n = 5). We conclude that synaptically released ATP, if exists, does not influence presynaptic A_1Rs.

Inhibition of GABA Release through A_1Rs and $GABA_B$Rs is Additive in Control, but Occlusive in Case of Maximal Activation of either A_1Rs or $GABA_B$Rs

We have recently reported that tonically activated $GABA_B$ receptors inhibit GABA release in GABAergic synapses on CR cells (Kirmse and Kirischuk 2006a). Both A_1Rs and $GABA_B$Rs are coupled to a G-protein of G_o/G_i type. Therefore, the DPCPX-induced effects can result from a shift in tonic $GABA_B$R-mediated inhibition of GABA release. To examine the possibility, we applied DPCPX in the presence of CGP55845, a specific $GABA_B$R blocker, and recorded mIPSCs. CGP55845 (1 μM) increased mIPSC frequency from 0.04 ± 0.01 to 0.05 ± 0.03 (P < 0.05, n = 8). However, in the presence of CGP55845 DPCPX still was able to increase mIPSC frequency to 0.07 ± 0.01 (P < 0.05 to both, n = 8, data not shown). These data suggest that the DPCPX-induced increase of mIPSC frequency does not depend on presynaptic $GABA_B$R activity.

Next, we inspected the additivity of $GABA_B$R- and A_1R-mediated tonic inhibition of evoked release. Figure 8*A* shows that DPCPX affected eIPSCs even in the presence of CGP55845. The corresponding PPR values were 1.7 ± 0.2, 0.9 ± 0.1, and 0.6 ± 0.1 in control, in the presence of CGP55845 and CGP55845 plus DPCPX (P < 0.05, n = 9, ANOVA and post hoc Student's t-test, Fig. 8*B*). Similar results were obtained when A_1Rs were blocked firstly. The corresponding PPR values were 1.6 ± 0.2, 1.0 ± 0.1, and 0.6 ± 0.1 in control, in the presence of DPCPX and DPCPX plus CGP55845 (P < 0.05, n = 6, ANOVA and post hoc Student's t-test, Fig. 8*C*). These results suggest that tonic inhibition of GABA release is rather additively mediated via presynaptic A_1Rs and $GABA_B$Rs.

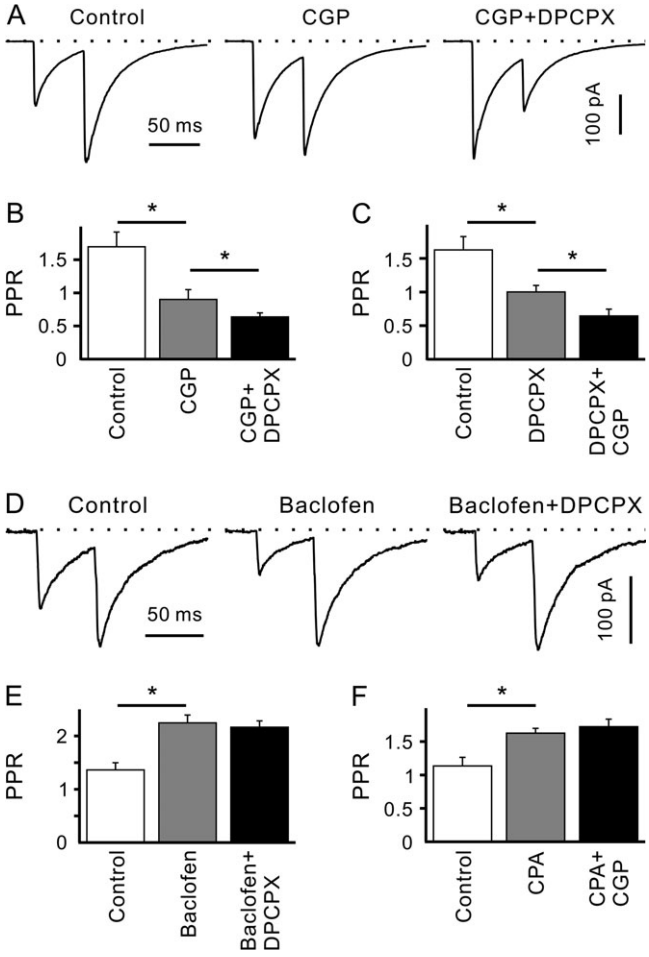

Figure 8. Convergent control of GABA release by presynaptic A_1Rs and $GABA_B$Rs. (*A*) Paired-pulse–induced eIPSCs in control, in the presence of CGP55845 (CGP, 1 μM) and CGP55845 plus DPCPX. Traces represent an average of 40 sequential responses. (*B*) Statistical data show that DPCPX significantly decreased the PPR when applied in the presence of CGP55845 (n = 9). (*C*) Statistical data show that CGP55845 significantly decreased the PPR when applied in the presence of DPCPX (n = 6). (*D*) Paired-pulse–induced eIPSCs in control, in the presence of baclofen (10 μM) and baclofen plus DPCPX. Traces represent an average of 40 sequential responses. (*E*) Statistical data show that DPCPX failed to affect the PPR when applied in the presence of baclofen (n = 5). (*F*) Statistical data show that CGP55845 did not influence the PPR when applied in the presence of CPA (n = 5). Symbol * shows a significant difference (P < 0.05).

Next, we tried to maximally activate $GABA_B$Rs or A_1Rs. Baclofen (10 μM), a specific $GABA_B$R agonist, significantly increased the PPR and abolished the DPCPX-mediated effects (Fig. 8*D*,*E*). The corresponding PPR values were 1.37 ± 0.13, 2.24 ± 0.14, and 2.17 ± 0.12 in control, in the presence of baclofen and baclofen plus DPCPX, respectively (P < 0.05 for control vs. baclofen and P > 0.4 for baclofen vs. baclofen plus DPCPX groups, n = 5, ANOVA and post hoc Student's t-test, Fig. 8*D*,*E*). Similar results were obtained when A_1Rs were activated

firstly. The corresponding PPR values were 1.13 ± 0.12, 1.63 ± 0.08, and 1.72 ± 0.11 in control, in the presence of CPA and CPA plus CGP55845, respectively ($P < 0.05$ for control vs. CPA and $P > 0.5$ for CPA vs. CPA plus CGP55845, $n = 5$, ANOVA and post hoc Student's t-test, Fig. 8*F*). These data show a functional convergence of the signaling pathways engaged by A_1Rs and $GABA_B$Rs.

Discussion

Our results show that the strength of excitatory GABAergic synapses in layer I is reduced during the first postnatal week. This developmental weakening of GABAergic transmission results from an A_1R-mediated decrease of GABA release probability. Presynaptic A_1Rs are upregulated between P2 and P5 and are tonically activated by endogenous adenosine derived from nonsynaptically released ATP.

Developmental Upregulation of A_1R-Mediated Inhibition of GABAergic Transmission

In rodents, GABAergic fibers in layer I can be traced already at E16 (Lauder et al. 1986). This plexus is presumably formed by axons of intrinsic GABAergic cells and afferent projections from the zona incerta of the ventral thalamus (Lin et al. 1990). Unfortunately, the exact origin of IPSCs recorded in this study can not be unequivocally elucidated. Projection neurons in the zona incerta are spontaneously active by the first postnatal week as revealed by cytochrome oxidase staining (Nicolelis et al. 1995) and electrophysiological investigations (Dammerman et al. 2000). Non-CR cells in layer I, presumably GABAergic neurons, are capable of repetitive firing (Zhou and Hablitz 1996) and display high frequency of spontaneous Ca^{2+} transients (Schwartz et al. 1998). Therefore, IPSCs recorded from CR cells may be generated by both populations of GABAergic neurons.

Spontaneous IPSCs have been observed in rat CR cells already at P0 showing that GABAergic synapses are functional at birth (Kilb and Luhmann 2001). As in other cortical cells (Luhmann and Prince 1991; Owens et al. 1996), GABA has a depolarizing effect on CR cells (Mienville 1998). Consequently, GABAergic IPSCs are potentially capable to elicit action potentials in CR cells. Indeed, GABA-driven, action-potential–dependent correlated neuronal network activity was observed in CR cells using optical recordings from an isolated hemisphere preparation (Aguilo et al. 1999). Interestingly, both groups reported a strong decrease of the frequency of spontaneous IPSCs (Kilb and Luhmann 2001) or Ca^{2+} transients (Schwartz et al. 1998) after P4. Our data indicate that an upregulation of presynaptic A_1Rs during the first postnatal week may underlie these developmental changes.

This suggestion is based on the following results. At P5–7 DPCPX strongly increased the mean eIPSC amplitude and decreased PPR, whereas CPA demonstrated the opposite. In addition, DPCPX increased the frequency of mIPSCs without affecting the median mIPSC amplitude. The latter and lack of either DPCPX or CPA effects on the resting potential and/or membrane resistance argues against the postsynaptic site of A_1R-mediated effects. In contrast to the results obtained at P5–7, both DPCPX and CPA only marginally affected GABAergic transmission at P1–2 showing that presynaptic A_1Rs are either not expressed or not functional at this age. These results are in agreement with previous observations reporting that adenosinergic system matures at early postnatal ages. Expression of A_1Rs has been shown to be low in fetuses and increases during the first 2 postnatal weeks (Geiger et al. 1984; Rivkees 1995; Aden et al. 2001). In addition, postnatal upregulation of A_1Rs is accompanied by a significant increase in extracellular adenosine concentration (Aranda et al. 1989).

Interestingly, A_1Rs appear to be only partially activated by endogenous adenosine at P5–7. Estimates of basal extracellular concentration of adenosine are in the range of 25–500 nM (Ballarin et al. 1991; Dunwiddie and Diao 1994). Given the high affinity (about 70 nM) of adenosine for A_1Rs, the latter could be fully activated at rest that would lead to a constant inhibition of excitatory GABAergic transmission. However, this seems to be not the case at P5–7, because A_1R activation with CPA is able to strengthen the A_1R-mediated inhibition of GABA release (Fig. 4). Consequently, further increase of adenosine concentration can lead to a stronger suppression of GABAergic transmission.

Cross-talk between Presynaptic $GABA_B$ and Adenosine A_1 Receptors

In contrast to adenosinergic system, tonic $GABA_B$R-mediated inhibition of GABA release was observed both at P1–2 (our unpublished data) and P5–7 (Kirmse and Kirischuk 2006a). However, PPR in controls was significantly larger at P5–7 (Fig. 2) than at P1–2 (Fig. 5), suggesting a developmental decrease of GABA release probability (calculated p_r, 0.22 at P1–2 and 0.13 at P5–7). Blockade of $GABA_B$Rs did not eliminate the observed difference (p_r, 0.41 at P1–2 and 0.31 at P5–7). Thus, at P5–7 tonic A_1R-mediated inhibition does not replace or duplicate the $GABA_B$R-mediated ones, but rather it contributes additively to the earlier-occurring $GABA_B$R-mediated depression of GABA release.

Adenosine A_1Rs as well as $GABA_B$Rs are coupled to pertussis toxin–sensitive G proteins. In line with this, NEM, a $G_{i/o}$-protein uncoupler, abolished both $GABA_B$R- (Kirmse and Kirischuk 2006b) and A_1R-mediated (our unpublished data) inhibition of GABA release. Because both receptor types share, at least partly, a common signaling pathway, an important issue is to know whether full activation of one type would occlude the action of the other. It seems to be the case, because baclofen completely abolished the DPCPX effects on eIPSCs and, vice versa, CPA entirely blocked the CGP55845 actions. These data show that the density of presynaptic A_1Rs at P5–7 is already high. Therefore, the A_1R-mediated inhibition of GABA release can become decisive provided a further increase of extracellular adenosine concentration, for instance during postnatal development (Aranda et al. 1989), takes place.

Extracellular ATP Degradation as the Main Source of Adenosine

In this context, it is of importance to examine the factors governing extracellular adenosine concentration. There are 2 primary mechanisms by which adenosine can reach the extracellular space: 1) it can be released via bidirectional equilibrative nucleoside transporters (ENTs, King et al. 2006); 2) it can be generated extracellular by the metabolism of released nucleotides (for review see Dunwiddie and Masino 2001; Sawynok and Liu 2003). Two forms of ENT (ENT1 and ENT2) are present in the CNS. In this study dipyridamole, a blocker of both types of adenosine transporters (Kiss et al. 2000), failed to influence either the mean amplitude of eIPSCs or the PPR suggesting that ENTs do not release adenosine under

control conditions. In contrast to dipyridamole, both AMPCP, an ecto-5′-nucleotidase antagonist, and ARL-67156, an ecto-ATPase inhibitor, completely abolished the DPCPX effects on GABA release. This data suggests that adenosine is generated extracellularly from adenine nucleotides. It is worth mentioning that ARL-67156 inhibits dephosphorylation of ATP to adenosine diphosphate (ADP) (Crack et al. 1995), whereas AMPCP blocks the conversion of adenosine monophosphate (AMP) to adenosine. Because ARL-67156 abolishes the AMPCP effects, we conclude that ATP, but not ADP or AMP, is the main source of extracellular adenosine.

ATP is present in all intracellular organelles, including synaptic vesicles, and calcium-dependent ATP release was observed in synaptosomes from specific brain regions including cortex (White et al. 1980). Moreover, corelease of GABA and ATP has been shown from cultured spinal and hypothalamic neurons (Jo and Schlichter 1999; Jo and Role 2002). However, the following data argue against the suggestion that ATP is released synaptically. Firstly, DPCPX failed to affect the PPR at long (250–1000 ms) ISIs. Secondly, in the presence of CGP55845 we did not find any correlation between individual eIPSCs in pairs. Such a correlation could be considered to reflect a release-dependent correlation between 2 eIPSCs like in the case of presynaptic $GABA_B$Rs in the same preparation (Kirmse and Kirischuk 2006a). Thirdly, both high (20 Hz, Fig. 2*E*) and low (4 Hz, Fig. 7*D*) frequency stimulations failed to influence the tetanic suppression of eIPSC amplitude suggesting that activity-dependent accumulation of adenosine in the vicinity of GABAergic synapses did not occur (Cunha et al. 1996). Taken together, our data allow suggesting that synaptic corelease of GABA and ATP does not take place in this preparation.

Besides exocytosis, ATP can be released via alternative routes including gap junction hemi-channels, volume-sensitive Cl^- channels, or $P2X_7$ receptors (Stout et al. 2002; Darby et al. 2003; Suadicani et al. 2006). One can speculate that ATP originates from glial cells (for review Fields and Burnstock 2006). ATP release from glial cells has been shown to result in A_1R-mediated inhibition of neurons, for instance, in the retina (Newman 2003) and in the hippocampus (Pascual et al. 2005). In the developing neocortex, ATP release–dependent calcium waves propagating through radial glial cells have been shown to influence cell proliferation (Weissman et al. 2004). Therefore, an ATP/adenosine-mediated glia-neuron interaction might occur also in layer I.

Physiological Significance

Due to the high input resistance of CR cells, GABAergic IPSCs may produce a prominent membrane depolarization and elicit action potentials (Zhou and Hablitz 1996; Kilb and Luhmann 2001). Axonal collaterals of CR cells project over >2 mm of cortical surface and make many synaptic (chemical and electrical) contacts presumably with terminal tuft dendrites of pyramidal neurons (Radnikow et al. 2002). Interestingly, incertocortical axons have been reported to make synaptic contacts on the apical dendrites of pyramidal cells (Dammerman et al. 2000). Moreover, both individual incertocortical and CR cell axons are capable to contact multiple pyramidal neurons. If the populations of pyramidal neurons innervated by incertocortical projections and CR cells overlap, simultaneous activity of incertocortical input and CR cells will result in a stronger depolarization in a specific subset of pyramidal neurons. As many thalamocortical synapses lack synaptic non-NMDA glutamate receptors during the first postnatal week and are functionally silent at negative membrane potentials (Isaac et al. 1997), the depolarization in layer I may support an activity-dependent refinement of thalamocortical circuitry.

It is tempting to speculate that the observed downregulation of excitatory GABAergic transmission by adenosinergic system may reflect an important phase of a complex process of the corticogenesis governed by CR cells and radial glia. The following hypothetical scenario could be suggested. Firstly, reelin secreted by CR cells shapes the morphology of radial glia cells thereby organizing a scaffold for radial cell migration (Hartfuss et al. 2003). Secondly, radial glial cells partly via ATP release govern cell proliferation and migration (Weissman et al. 2004). At this stage, GABAergic synapses in layer I do not express A_1Rs, therefore, in addition to reelin secretion, electrical activity of CR cells may depolarize neuronal cells in the cortical plate influencing thereby glutamatergic synaptogenesis. Finally, when glutamatergic synapses are formed, ATP released from radial glia serves as a source of adenosine. The latter inhibits or may be even terminate excitatory GABAergic transmission in layer I. Hypothetically, an A_1R-mediated "switch-off" of synaptic inputs to CR cells may also have the consequence that CR cells disappear by the end of the second postnatal week.

Notes

The technical assistance of Mrs Kerstin Rückwardt is highly appreciated. This study was supported by German Research Council (Deutsche Forschungsgemeinschaft, DFG, GR986/9-1 and KI1093/1-1 to SK). K.K. has received a scholarship from DFG as a member of the Graduate School (Graduiertenkolleg 238). *Conflict of Interest*: None declared.

Address correspondence to Dr Sergei Kirischuk, Institute of Neurophysiology, Johannes-Mueller-Center of Physiology, Charité-University-Medicine Berlin, Tucholskystr. 2, 10117 Berlin, Germany. Email: sergei.kirischuk@charite.de.

References

Aden U, Leverin AL, Hagberg H, Fredholm BB. 2001. Adenosine A(1) receptor agonism in the immature rat brain and heart. Eur J Pharmacol. 426:185–192.

Aguilo A, Schwartz TH, Kumar VS, Peterlin ZA, Tsiola A, Soriano E, Yuste R. 1999. Involvement of Cajal-Retzius neurons in spontaneous correlated activity of embryonic and postnatal layer 1 from wild-type and Reeler mice. J Neurosci. 19:10856–10868.

Aranda JV, Beharry K, Laudignon N, Sasyniuk BI. 1989. Ontogeny of adenosine production and degradation and its implications in neonatal cerebral blood flow regulation. Dev Pharmacol Ther. 13:96–103.

Ballarin M, Fredholm BB, Ambrosio S, Mahy N. 1991. Extracellular levels of adenosine and its metabolites in the striatum of awake rats: inhibition of uptake and metabolism. Acta Physiol Scand. 142:97–103.

Connors BW, Prince DA. 1982. Effects of local anesthetic QX-314 on the membrane properties of hippocampal pyramidal neurons. J Pharmacol Exp Ther. 220:476–481.

Crack BE, Pollard CE, Beukers MW, Roberts SM, Hunt SF, Ingall AH, McKechnie KC, IJzerman AP, Leff P. 1995. Pharmacological and biochemical analysis of FPL 67156, a novel, selective inhibitor of ecto-ATPase. Br J Pharmacol. 114:475–481.

Cunha RA. 2001. Adenosine as a neuromodulator and as a homeostatic regulator in the nervous system: different roles, different sources and different receptors. Neurochem Int. 38:107–125.

Cunha RA, Vizi ES, Ribeiro JA, Sebastiao AM. 1996. Preferential release of ATP and its extracellular catabolism as a source of adenosine upon high- but not low-frequency stimulation of rat hippocampal slices. J Neurochem. 67:2180–2187.

Dammerman RS, Flint AC, Noctor S, Kriegstein AR. 2000. An excitatory GABAergic plexus in developing neocortical layer 1. J Neurophysiol. 84:428–434.
Darby M, Kuzmiski JB, Panenka W, Feighan D, MacVicar BA. 2003. ATP released from astrocytes during swelling activates chloride channels. J Neurophysiol. 89:1870–1877.
Deckert J, Morgan PF, Marangos PJ. 1988. Adenosine uptake site heterogeneity in the mammalian CNS? Uptake inhibitors as probes and potential neuropharmaceuticals. Life Sci. 42:1331–1345.
Dunwiddie TV, Diao L. 1994. Extracellular adenosine concentrations in hippocampal brain slices and the tonic inhibitory modulation of evoked excitatory responses. J Pharmacol Exp Ther. 268:537–545.
Dunwiddie TV, Diao L, Proctor WR. 1997. Adenine nucleotides undergo rapid, quantitative conversion to adenosine in the extracellular space in rat hippocampus. J Neurosci. 17:7673–7682.
Dunwiddie TV, Masino SA. 2001. The role and regulation of adenosine in the central nervous system. Annu Rev Neurosci. 24:31–55.
Fastbom J, Pazos A, Palacios JM. 1987. The distribution of adenosine A_1 receptors and 5′-nucleotidase in the brain of some commonly used experimental animals. Neuroscience. 22:813–826.
Fields RD, Burnstock G. 2006. Purinergic signalling in neuron-glia interactions. Nat Rev Neurosci. 7:423–436.
Fredholm BB, Chen JF, Cunha RA, Svenningsson P, Vaugeois JM. 2005. Adenosine and brain function. Int Rev Neurobiol. 63:191–270.
Frotscher M. 1998. Cajal-Retzius cells, Reelin, and the formation of layers. Curr Opin Neurobiol. 8:570–575.
Geiger JD, LaBella FS, Nagy JI. 1984. Ontogenesis of adenosine receptors in the central nervous system of the rat. Brain Res. 315:97–104.
Hartfuss E, Forster E, Bock HH, Hack MA, Leprince P, Luque JM, Herz J, Frotscher M, Gotz M. 2003. Reelin signaling directly affects radial glia morphology and biochemical maturation. Development. 130: 4597–4609.
Hestrin S, Armstrong WE. 1996. Morphology and physiology of cortical neurons in layer I. J Neurosci. 16:5290–5300.
Hugel S, Schlichter R. 2003. Convergent control of synaptic GABA release from rat dorsal horn neurones by adenosine and GABA autoreceptors. J Physiol. 551:479–489.
Isaac JT, Crair MC, Nicoll RA, Malenka RC. 1997. Silent synapses during development of thalamocortical inputs. Neuron. 18:269–280.
Jo YH, Role LW. 2002. Coordinate release of ATP and GABA at in vitro synapses of lateral hypothalamic neurons. J Neurosci. 22:4794–4804.
Jo YH, Schlichter R. 1999. Synaptic corelease of ATP and GABA in cultured spinal neurons. Nat Neurosci. 2:241–245.
Kilb W, Luhmann HJ. 2000. Characterization of a hyperpolarization-activated inward current in Cajal-Retzius cells in rat neonatal neocortex. J Neurophysiol. 84:1681–1691.
Kilb W, Luhmann HJ. 2001. Spontaneous GABAergic postsynaptic currents in Cajal-Retzius cells in neonatal rat cerebral cortex. Eur J Neurosci. 13:1387–1390.
King AE, Ackley MA, Cass CE, Young JD, Baldwin SA. 2006. Nucleoside transporters: from scavengers to novel therapeutic targets. Trends Pharmacol Sci. 27:416–425.
Kirischuk S, Grantyn R. 2003. Intraterminal Ca2+ concentration and asynchronous release at single GABAergic boutons in rat collicular cultures. J Physiol. 548:753–764.
Kirmse K, Kirischuk S. 2006a. Ambient GABA constrains the strength of GABAergic synapses at Cajal-Retzius cells in the developing visual cortex. J Neurosci. 26:4216–4227.
Kirmse K, Kirischuk S. 2006b. N-ethylmaleimide increases release probability at GABAergic synapses in layer I of the mouse visual cortex. Eur J Neurosci. 24:2741–2748.
Kiss A, Farah K, Kim J, Garriock RJ, Drysdale TA, Hammond JR. 2000. Molecular cloning and functional characterization of inhibitor-sensitive (mENT1) and inhibitor-resistant (mENT2) equilibrative nucleoside transporters from mouse brain. Biochem J. 352:363–372.
Lauder JM, Han VK, Henderson P, Verdoorn T, Towle AC. 1986. Prenatal ontogeny of the GABAergic system in the rat brain: an immunocytochemical study. Neuroscience. 19:465–493.
Lin CS, Nicolelis MA, Schneider JS, Chapin JK. 1990. A major direct GABAergic pathway from zona incerta to neocortex. Science. 248:1553–1556.
Lu T, Trussell LO. 2000. Inhibitory transmission mediated by asynchronous transmitter release. Neuron. 26:683–694.
Luhmann HJ, Prince DA. 1991. Postnatal maturation of the GABAergic system in rat neocortex. J Neurophysiol. 65:247–263.
Marin-Padilla M. 1998. Cajal-Retzius cells and the development of the neocortex. Trends Neurosci. 21:64–71.
Mienville JM. 1998. Persistent depolarizing action of GABA in rat Cajal-Retzius cells. J Physiol. 512:809–817.
Mienville JM, Pesold C. 1999. Low resting potential and postnatal upregulation of NMDA receptors may cause Cajal-Retzius cell death. J Neurosci. 19:1636–1646.
Newman EA. 2003. Glial cell inhibition of neurons by release of ATP. J Neurosci. 23:1659–1666.
Nicolelis MA, Chapin JK, Lin RC. 1995. Development of direct GABAergic projections from the zona incerta to the somatosensory cortex of the rat. Neuroscience. 65:609–631.
Owens DF, Boyce LH, Davis MB, Kriegstein AR. 1996. Excitatory GABA responses in embryonic and neonatal cortical slices demonstrated by gramicidin perforated-patch recordings and calcium imaging. J Neurosci. 16:6414–6423.
Pascual O, Casper KB, Kubera C, Zhang J, Revilla-Sanchez R, Sul JY, Takano H, Moss SJ, McCarthy K, Haydon PG. 2005. Astrocytic purinergic signaling coordinates synaptic networks. Science. 310: 113–116.
Radnikow G, Feldmeyer D, Lubke J. 2002. Axonal projection, input and output synapses, and synaptic physiology of Cajal-Retzius cells in the developing rat neocortex. J Neurosci. 22:6908–6919.
Reppert SM, Weaver DR, Stehle JH, Rivkees SA. 1991. Molecular cloning and characterization of a rat rat A_1-adenosine receptor that is widely expressed in brain and spinal cord. Mol Endocrinol. 5:1037–1048.
Retzius G. 1893. Die Cajalschen Zellen der Grosshirnrinde beim Menschen und bei Saugetieren. Biol Untersuch. 5:1–9.
Ribeiro JA, Sebastiao AM, de Mendonca A. 2002. Adenosine receptors in the nervous system: pathophysiological implications. Prog Neurobiol. 68:377–392.
Rivkees SA. 1995. The ontogeny of cardiac and neural A1 adenosine receptor expression in rats. Brain Res Dev Brain Res. 89:202–213.
Sawynok J, Liu XJ. 2003. Adenosine in the spinal cord and periphery: release and regulation of pain. Prog Neurobiol. 69:313–340.
Schneggenburger R, Meyer AC, Neher E. 1999. Released fraction and total size of a pool of immediately available transmitter quanta at a calyx synapse. Neuron. 23:399–409.
Schwartz TH, Rabinowitz D, Unni V, Kumar VS, Smetters DK, Tsiola A, Yuste R. 1998. Networks of coactive neurons in developing layer 1. Neuron. 20:541–552.
Stout CE, Costantin JL, Naus CC, Charles AC. 2002. Intercellular calcium signaling in astrocytes via ATP release through connexin hemichannels. J Biol Chem. 277:10482–10488.
Suadicani SO, Brosnan CF, Scemes E. 2006. P2X7 receptors mediate ATP release and amplification of astrocytic intercellular Ca2+ signaling. J Neurosci. 26:1378–1385.
Weaver DR. 1996. A1-adenosine receptor gene expression in fetal rat brain. Brain Res Dev Brain Res. 94:205–223.
Weissman TA, Riquelme PA, Ivic L, Flint AC, Kriegstein AR. 2004. Calcium waves propagate through radial glial cells and modulate proliferation in the developing neocortex. Neuron. 43:647–661.
White T, Potter P, Wonnacott S. 1980. Depolarisation-induced release of ATP from cortical synaptosomes is not associated with acetylcholine release. J Neurochem. 34:1109–1112.
Zhou FM, Hablitz JJ. 1996. Postnatal development of membrane properties of layer I neurons in rat neocortex. J Neurosci. 16: 1131–1139.
Zimmermann H. 2000. Extracellular metabolism of ATP and other nucleotides. Naunyn Schmiedebergs Arch Pharmacol. 362:299–309.